Organometallics 1987, *6*, 2307–2313

Iridium- and Rhodium-Initiated C–C Coupling of Carbon Dioxide with Malonodinitrile

Arno Behr,*[†] Eberhardt Herdtweck,[‡] Wolfgang A. Herrmann,[‡] Wilhelm Keim,[†] and Walter Kipshagen[†]

Institut für Technische Chemie und Petrolchemie, Technische Universität Aachen, D-5100 Aachen, Germany, and Anorganisch Chemisches Institut der Technischen Universität München, D-8046 Garching, Germany

Received December 2, 1986

Electron-rich complexes of iridium(I) and rhodium(I) react with activated alkanes such as malonodinitrile and carbon dioxide under C–C coupling to give compounds of the general formula $[L_nMXH]^+[O_2CCH(CN)_2]^-$ (L = PMe_3, n = 4; L = dmpe or depe, n = 2; X = Cl, H; M = Ir, Rh). The influence of the different phosphorus ligands on the structures of the complexes is described. Compounds $[HIr(depe)_2Cl]^+[O_2CCH(CN)_2]^-$ (**1**) and $[H_2Ir(PMe_3)_4]^+[O_2CCH(CN)_2]^-$ (**4**) have been characterized by X-ray structure analyses which both show the dicyanoacetate anions to be dimeric via hydrogen bonds in the crystal form. To study the reaction mechanism the complexes $HIr(PMe_3)_4$ and $[Ir(depe)_2]Cl$ were reacted in the absence of carbon dioxide with malonodinitrile and yielded the C–H activated malonodinitrile anion complexes $[H_2Ir(PMe_3)_4]^+[CH(CN)_2]^-$ (**5**) (X-ray structure determination confirms the supposed molecular structure) and $[HIr(depe)_2Cl]^+[CH(CN)_2]^-$ (**6**). Reaction of **5** with CO_2 yields quantitatively **4** under mild reaction conditions.

Introduction

In recent years, great efforts have been made to find alternative raw materials for organic synthesis. Carbon dioxide as well as alkanes are available as potential carbon sources for the future, but their great disadvantage, however, is their inertness in chemical reactions. Recent experiments to activate paraffins and to coordinate carbon dioxide have shown transition-metal chemistry to have overcome this inertness.

Coordination chemistry of carbon dioxide is a field of growing interest in organometallic chemistry.[1] Only a few complexes with carbon dioxide as a ligand are known,[2] but there are many examples of insertion reactions of CO_2 into M–H and M–C bonds of transition-metal complexes. Since the insertion into the metal–carbon bond is a necessary step in using CO_2 as a source of chemical carbon, stoichiometric and catalytic C–C coupling reactions with CO_2 have attracted considerable attention during the past years and are also a topic of the work in our group.[3]

Carbon–hydrogen bond activation by transition-metal complexes has been of interest for about 20 years.[4] The first example of an intermolecular sp^3 C–H bond activation, described in 1965,[5] was followed by a number of publications describing the intramolecular activation of C–H bond,[6] a much more frequent procedure than intermolecular reactions.[7] Simple alkanes are hardly attacked by transition-metal complexes, whereas alkyl–C–H bonds activated by electron-withdrawing substituents[8] react rapidly.

One interesting approach is the direct carboxylation of alkanes. Intramolecular reactions with insertion of CO_2 into a metal–carbon bond of a coordinated ligand are well-known.[9] Intermolecular reactions have also been reported; for instance, the complex $HFe(dmpe)_2Np$ (Np = 2-naphthyl substituent), which produces $HFe(CH_2CN)(dmpe)_2$ in acetonitrile, and CO_2 lead to the formation of a cyanoacetate complex that was characterized in solution by spectroscopical means[10] (eq 1). Electron-rich iridium complexes react in a similar way. $[Ir(depe)_2]Cl$ dissolves in acetonitrile to produce [HIr-

$$HFe(dmpe)_2Np + CH_3CN \rightarrow HFe(CH_2CN)(dmpe)_2 + HNp$$

$$HFe(CH_2CN)(dmpe)_2 + CO_2 \rightarrow HFe(O_2CCH_2CN)(dmpe)_2 \quad (1)$$

[†] Technische Universität Aachen.

[‡] Technische Universität München.

(1) (a) Behr, A. In *Catalysis in C_1 Chemistry*; Keim, W., Ed.; Reidel Publishing Co.: Dordrecht, 1983; pp 169–217. (b) Behr, A. *Angew. Chem., Int. Ed. Engl.*, in press. (c) Darensbourg, D. J.; Kudaroski, R. A. *Adv. Organomet. Chem.* **1983**, *22*, 129. (d) Eisenberg, R.; Hendriksen, D. E. *Adv. Catal.* **1979**, *28*, 79. (e) Kolomnikov, I. S.; Grigoryan, M. Kh. *Russ. Chem. Rev. (Engl. Transl.)* **1978**, *47*, 334. (f) Inoue, S.; Yamazaki, N. *Organic and Bioorganic Chemistry of Carbon Dioxide*; Kodansha Ltd.: Tokyo, 1982.

(2) (a) Aresta, M.; Nobile, C. F.; Albano, V. G.; Forni, E.; Manassero, M. *J. Chem. Soc., Chem. Commun.* **1975**, 636. (b) Bristow, G. S.; Hitchcock, P. B.; Lappert, M. F. *J. Chem. Soc., Chem. Commun.* **1981**, 1145. (c) Fachinetti, G.; Floriani, C.; Zanazzi, P. F. *J. Am. Chem. Soc.* **1978**, *95*, 7405. (d) Calabrese, J. C.; Herskovitz, T.; Kinney, J. B. *J. Am. Chem. Soc.* **1983**, *105*, 5914. (e) Alvarez, R.; Carmona, E.; Gutierrez-Puebla, E.; Marin, J. M.; Monge, A.; Poveda, M. L. *J. Chem. Soc., Chem. Commun.* **1984**, 1326. (f) Gambarotta, S.; Floriani, C.; Chiesi-Villa, A.; Guastini, C. *J. Am. Chem. Soc.* **1985**, *107*, 2985. (g) Lundquist, E. G.; Huffman, J. C.; Caulton, K. G. *J. Am. Chem. Soc.* **1986**, *108*, 8309.

(3) For some examples see: (a) Behr, A.; He, R.; Juszak, K.-D.; Krüger, C.; Tsay, Y.-H. *Chem. Ber.* **1986**, *119*, 991. (b) Behr, A.; Kanne, U. *J. Organomet. Chem.* **1986**, *309*, 215. (c) Behr, A.; Thelen, G. *C_1 Mol. Chem.* **1984**, *1*, 137. (d) Behr, A.; Kanne, U.; Thelen, G. *J. Organomet. Chem.* **1984**, *269*, C1. (e) Behr, A.; He, R. *J. Organomet. Chem.* **1984**, *276*, C69. (f) Behr, A.; Juszak, K.-D. *J. Organomet. Chem.* **1983**, *255*, 263. (g) Behr, A.; Keim, W.; Thelen, G. *J. Organomet. Chem.* **1983**, *249*, C38. (h) Behr, A.; Juszak, K.-D.; Keim, W. *Synthesis* **1983**, 574.

(4) (a) Ephritikhine, M. *Nouv. J. Chim.* **1986**, *10*, 9. (b) Halpern, J. *Inorg. Chim. Acta* **1985**, *100*, 41. (c) Crabtree, R. H. *Chem. Rev.* **1985**, *85*, 245–269. (d) Rothwell, I. P. *Polyhedron* **1985**, *4*, 177. (e) Parshall, G. W.; Herskovitz, T.; Tebbe, F. N.; English, A. D.; Zeile, J. V. *Fundam. Res. Homogeneous Catal.* **1979**, *3*, 95. (f) Webster, D. E. *Adv. Organomet. Chem.* **1977**, *15*, 147. (g) Shilov, A. E.; Shteinman, A. A. *Coord. Chem. Rev.* **1977**, *24*, 97.

(5) (a) Chatt, J.; Davidson, J. M. *J. Chem. Soc.* **1965**, 843. (b) Cotton, F. A.; Frenz, B. A.; Hunter, D. L. *J. Chem. Soc., Chem. Commun.* **1974**, 755.

(6) For some reviews see: (a) Calabrese, J. C.; Colton, M. C.; Herskovitz, T.; Klabunde, U.; Parshall, G. W.; Thorn, D. L.; Tulip, T. H. *Ann. N.Y. Acad. Sci.* **1983**, *415*, 302. (b) Bruce, M. I. *Angew. Chem., Int. Ed. Engl.* **1977**, *16*, 73. (c) Parshall, G. W. *Acc. Chem. Res.* **1970**, *3*, 139.

(7) (a) Jones, W. D.; Maguire, J. A. *Organometallics* **1986**, *5*, 590. (b) Desrosiers, P. J.; Shinomoto, R. S.; Flood, T. C. *J. Am. Chem. Soc.* **1986**, *108*, 1346. (c) Bergman, R. G.; Seidler, P. F.; Wenzel, T. T. *J. Am. Chem. Soc.* **1985**, *107*, 4358. (d) Janowicz, A. H.; Periana, R. A.; Buchanan, M.; Kovac, C. A.; Stryker, J. M.; Wax, M. J.; Bergman, R. G. *Pure Appl. Chem.* **1984**, *56*, 13. (e) Hoyano, J. K.; McMaster, A. D.; Graham, W. A. G. *J. Am. Chem. Soc.* **1983**, *105*, 7190. (f) Watson, P. L. *J. Am. Chem. Soc.* **1983**, *105*, 6491.

(8) For some examples see: (a) McGhee, W. D.; Bergman, R. G. *J. Am. Chem. Soc.* **1986**, *108*, 5621. (b) Ittel, S. D.; Tolman, C. A.; English, A. D.; Jesson, J. P. *J. Am. Chem. Soc.* **1976**, *98*, 6073. (c) Bennet, M. A.; Robertson, G. B.; Whimp, P. O.; Yoshida, T. *J. Am. Chem. Soc.* **1973**, *95*, 3028.

(9) (a) Herskovitz, T. *J. Am. Chem. Soc.* **1977**, *99*, 2391. (b) Karsch, H. H. *Chem. Ber.* **1977**, *110*, 2213.

0276-7333/87/2306-2307$01.50/0

Table I. Analytical Data of Complexes 1-6

	elemental anal. calcd (found)			
complex	C	H	N	O
1	38.42 (38.50)	6.72 (6.82)	3.73 (3.93)	4.27 (3.78)
2	nd[a]			
3	35.02 (36.73)	6.25 (6.36)	5.11 (5.37)	5.83 (5.60)
4	31.62 (31.76)	6.47 (6.50)	4.61 (4.40)	5.27 (5.17)
5	31.97 (31.29)	6.97 (6.90)	4.97 (4.82)	
6	39.12 (38.96)	7.14 (7.45)	3.97 (3.83)	

[a] nd = not determined.

Table II. Mass Spectra of Complexes 1-6

complex	mass spectra, *m/e*	yield, %
1	603, 581, 548, 513, 339, 337, 256, 177, 66, 18	74
2	479, 478, 402, 296, 294, 194, 186, 78, 66, 44	70
3	438, 402, 253, 151, 66, 44	58
4	487, 420, 419, 404, 389, 343, 76, 66, 61, 44	60
5	486, 423, 421, 419, 313, 311, 76, 66, 61, 59	64
6	603, 536, 339, 281, 256, 177, 66	37

$(CH_2CN)(depe)_2]Cl$. After pressuring with CO_2, the colorless solution obtained seems to contain the carboxylate complex $[HIr(O_2CCH_2CN)(depe)_2]Cl$ (eq 2).[11] With these

$$[Ir(depe)_2]Cl + CH_3CN \rightarrow [HIr(CH_2CN)(depe)_2]Cl$$

$$[HIr(CH_2CN)(depe)_2]Cl + CO_2 \rightarrow [HIr(O_2CCH_2CN)(depe)_2]Cl \quad (2)$$

examples in mind we reacted the activated C–H bond of malonodinitrile together with CO_2 and electron-rich complexes of iridium and rhodium. First results were published in a short communication,[12] more detailed results will be given here.

Experimental Section

^1H NMR spectra were recorded at 80 MHz on a Bruker Model WP 80 or at 200 MHz on a Bruker Model CXP 200 NMR spectrometer with DMSO-d_6 being used as a solvent and the shifts expressed as δ values relative to Me_4Si. The ^{13}C NMR and ^{31}P NMR spectra were recorded on the Bruker Model CXP 200 spectrometer. In ^{13}C NMR spectroscopy DMSO-d_6 was used as the internal standard; in ^{31}P NMR spectroscopy 85% phosphoric acid was used as the external standard. The IR spectra were measured on a Perkin-Elmer 782 spectrophotometer with a PE 3600 data station using KBr pellets. Mass spectra were recorded on a Varian MAT 112 instrument combined with the Varian Spectro System MAT 188 by using an ion source with a temperature of 210 °C, a pressure of 10^{-6} torr, and an ionization energy of 70 eV. Elemental analyses were carried out on a Carlo Erba 1106 elemental analyzer.

The starting complexes were prepared by methods described in the literature: $[Ir(dmpe)_2]Cl$,[13] $[Ir(depe)_2]Cl$,[14] $HIr(PMe_3)_4$,[15] and $[Rh(dmpe)_2]Cl$.[14] The ligands dmpe and depe were commercially available (Alfa Products), and PMe_3 was prepared according to ref 16. Solvents were dried by standard methods and were stored under argon. All operations were performed by using the Schlenk technique.

The reactions with CO_2 were carried out in a 80-mL steel autoclave at a pressure of 50 bar and a temperature of 50 °C. For the reactions with $[Ir(dmpe)_2]Cl$, $[Ir(depe)_2]Cl$, and $[Rh(dmpe)_2]Cl$ benzonitrile was used as a solvent, and THF was used for reactions with $HIr(PMe_3)_4$.

Preparation of Complexes 1-3. In a typical example the synthesis of complex 1 is described in detail. $[Ir(depe)_2]Cl$ (0.58 g, 0.91 mmol) was dissolved in 10 mL of benzonitrile. Malonodinitrile (0.0598 g, 0.91 mmol) in 10 mL of benzonitrile was stirred

Table III. IR Data of Complexes 1-6

complex	IR data, cm^{-1}
1	2195, 2174, 2135 [$\nu(C{\equiv}N)$]; 2116, 2080 [$\nu(Ir{-}H)$]; 1610, 1335 ($C{=}O$); 1030 ($P{-}C$)
2	2186, 2167, 2154 [$\nu(C{\equiv}N)$]; 2109, 2083 (sh) [$\nu(Ir{-}H)$]; 1606, 1313 ($C{=}O$); 950, 936, 901 ($P{-}C$)
3	2196, 2170, 2143 [$\nu(C{\equiv}N)$]; 2080 [$\nu(Rh{-}H)$]; 1612, 1322 ($C{=}O$); 952, 933, 900 ($P{-}C$)
4	2197, 2173, 2142 [$\nu(C{\equiv}N)$]; 2058, 2034 ν ($Ir{-}H$); 1612, 1330 ($C{=}O$); 946 ($P{-}C$)
5	2156, 2115, 2086 [$\nu(C{\equiv}N)$]; 2055, 2023 [$\nu(Ir{-}H)$]; 952 ($P{-}C$)
6	2298, 2204, 2156 [$\nu(C{\equiv}N)$]; 2114, 2078 [$\nu(Ir{-}H)$]; 1092, 1027 ($P{-}C$)

Table IV. ^1H NMR Data of Complexes 1-6

complex	^1H NMR data, δ
1	–22.35 (1 H, q, *J* = 12.8 Hz); 0.95 (12 H, t, *J* = 7.9 Hz); 1.13 (12 H, t, *J* = 7.9 Hz); 1.68 (4 H, m); 1.86 (12 H, m); 2.16 (4 H, m); 2.33 (4 H, m)
2	–22.73 (q, *J* = 14.2 Hz); –15.05[a] (m, *J* = 17.1 Hz); –14.50[a] (m, *J* = 17.1 Hz); 1.64[a] (12 H, s); 1.67 (12 H, s); 1.76[a] (12 H, s); 1.77 (12 H, s); 1.92[a] (8 H, s, br); 1.94 (8 H, tr, *J* = 8.9 Hz); 9.5[a] (br)
3	–18.48 (1 H, dq, J_q = 15.9 Hz, J_d = 24.2 Hz); 1.60 (24 H, s); 1.97 (8 H, s), 3.35 (s), 9.93 (br)
4	–13.29 (1 H, t, *J* = 21 Hz); –12.79 (1 H, tr, *J* = 21 Hz); 1.62 (18 Hz, d, *J* = 7.8 Hz); 1.70 (18 H, distorted t, *J* = 3.5 Hz)
5	–13.29 (1 H, t, *J* = 22 Hz); –12.80 (1 H, t, *J* = 22 Hz); 1.62 (18 H, d, *J* = 7.7 Hz); 1.69 (18 H, distorted t, *J* = 3.5 Hz)
6	–22.35 (1 H, q, *J* = 12.8 Hz); 0.95 (12 H, t, *J* = 7.9 Hz); 1.13 (12 H, t, *J* = 7.9 Hz); 1.68 (4 H, m); 1.86 (12 H, m); 2.17 (4 H, m); 2.3 (4 H, m); 3.34 (1 H, s)

[a] Signals disappear at a temperature of 100 °C.

Table V. ^{13}C NMR Data of Complexes 1-6

complex	^{13}C NMR data, δ
1	171.0 (carboxylate C); 133.3, 132.1, 129.4 (benzonitrile); 122.6 (nitrile C); 30.3 (methyne C); 20.9 (q, *J* = 17.7 Hz, bridge C); 19.5 (q, *J* = 8.9 Hz, alkyl CH_2); 16.2 (q, *J* = 8.9 Hz, alkyl CH_2); 8.8 (methyl C); 7.9 (methyl C)
2	171.0 (carboxylate C); 133.3, 132.1, 129.4 (benzonitrile); 122.7 (nitrile C); 30.3 (methyne C); 29.5[a] (m), 28.1 (q, *J* = 14 Hz, bridge C); 23.1[a] (m); 17.6 (q, *J* = 10.3 Hz, methyl C); 15.7[a] (m); 10.2 (q, *J* = 9.6 Hz, methyl C)
3	171.0 (carboxylate C); 133.3, 132.1, 129.4 (benzonitrile); 122.7 (nitrile C); 30.5 (methyne C); 28.0 (q, *J* = 13.3 Hz, bridge C); 17.0 (q, *J* = 7.9 Hz, methyl C); 11.7 (q, *J* = 7.9 Hz, methyl C)
4	171.7 (carboxylate C); 123.2 (nitrile C); 30.5 (methyne C); 25.0 (tr, *J* = 20.1 Hz, trans methyl C); 22.0 (filled d, cis methyl C)
5	130.2 (nitrile C); 25.0 (tr, *J* = 20.1 Hz, trans methyl); 22.0 (filled d, cis methyl); –1.9 (methyne anion C)
6	130.1 (nitrile C); 20.9 (q, *J* = 12.8 Hz bridge C); 19.5 (q, *J* = 9 Hz, alkyl CH_2); 16.2 (q, *J* = 9 Hz, alkyl CH_2); 8.8 (s, methyl C); 7.9 (s, methyl C); –2.0 (methyne anion C)

[a] Signals disappear at a temperature at 100 °C.

Table VI. ^{31}P NMR Data of Complexes 1-6

complex	^{31}P NMR data, δ
1	29.18 (s)
2	9.23 (s) (100 °C)
3	39.59 (d, *J* = 89 Hz)
4	–51.33 (t, *J* = 20.1 Hz), –57.33 (t, *J* = 20.1 Hz)
5	–51.37 (t, *J* = 20.1 Hz), –57.35 (t, *J* = 20.1 Hz)
6	30.13 (s)

---

(10) Ittel, S. D.; Tolman, C. A.; English, A. D.; Jesson, J. P. *J. Am. Chem. Soc.* **1978**, *100*, 7577.

(11) (a) English, A. D.; Herskovitz, T. *J. Am. Chem. Soc.* **1977**, *99*, 1648. (b) Parshall, G. W. *Catalysis* **1977**, *1*, 335.

(12) Behr, A.; Herdtweck, E.; Herrmann, W. A.; Keim, W.; Kipshagen, W. *J. Chem. Soc., Chem. Commun.* **1986**, 1262.

(13) Herskovitz, T. *Inorg. Synth.* **1982**, *21*, 99.

(14) Herskovitz, T.; Parshall, G. W. U.S. Patent 3954821, 1976.

(15) Thorn, D. L.; Tulip, D. L. *Organometallics* **1982**, *1*, 1580.

(16) Wolfsberger, W.; Schmidbaur, H. *Synth. React. Inorg. Met.-Org. Chem.* **1974**, *4*, 149.

Table VII. Crystal and Refinement Data for Complexes 1 and 4

formula	$C_{24}H_{50}ClIrN_2O_2P_4 \cdot {}^1/_2C_7H_5N$ (Z = 2) $C_{55}H_{105}Cl_2Ir_2N_5O_4P_8$ (Z = 1)	$C_{16}H_{39}IrN_2O_2P_4$
size and color	colorless, irregular crystals	light yellow tablets, 0.63 × 0.54 × 0.25 mm
mol wt	801.8 (Z = 2) 1603.6 (Z = 1)	607.6
cryst system	triclinic	triclinic
space group	$P\bar{1}$, IT No. 2	$P\bar{1}$, IT No. 2
a, pm	1053.3 (2)	973.8 (2)
b, pm	1409.5 (3)	1022.5 (2)
c, pm	1423.3 (3)	1331.0 (2)
α, deg	67.39 (2)	94.16 (2)
β, deg	67.30 (3)	92.04 (2)
γ, deg	84.97 (3)	95.27 (2)
V, pm^3	1795 × 10^6	1315 × 10^6
Z	2 or 1	2
temp, °C	22 ± 1	22 ± 1
D(calcd), g cm^{-3}	1.483	1.53
diffractometer	CAD 4 (Enraf-Nonius)	
radiation	graphite-monochromated Mo Kα (λ = 0.7107 Å)	
abs coeff, cm^{-1}	39.8	53.1
scan technique	ω	ω
scan width, deg	0.80 – 0.30 tan θ	
bkgd	25% of full scan width on both sides	
scan time	t_{max} = 60 s	
scan range, deg	2–17.5	1–22.5
measd data	2372	6790
unique data ($F_o > 3\sigma(F_o)$)	2061	3185
no. of refinement parameters	307	226
shift/err last cycle	0.05	0.00
$\Delta\bar{e}_0$/Å^3	1.7 at benzonitrile	2.1, 94 pm from Ir
GOF	3.783	3.343
R_F	0.041	0.050
R_{wF}	0.053	0.061

Table VIII. Positional Parameters of Complex 1 and Their Estimated Standard Deviations[a]

atom	x	y	z	B, Å^2
Ir	0.36778 (7)	0.23980 (5)	0.33333 (5)	3.07 (2)
Cl	0.3072 (5)	0.0643 (3)	0.4842 (3)	4.8 (1)
P1	0.1631 (5)	0.2975 (3)	0.4281 (3)	4.0 (1)
P2	0.2354 (5)	0.1956 (4)	0.2550 (4)	4.5 (1)
P3	0.4994 (5)	0.2933 (4)	0.4060 (3)	4.0 (1)
P4	0.5780 (5)	0.1898 (4)	0.2341 (3)	4.0 (1)
O1	–0.054 (1)	0.471 (1)	0.135 (1)	6.2 (4)
O2	–0.026 (1)	0.625 (1)	–0.007 (1)	6.8 (4)
N1	–0.191 (2)	0.514 (2)	0.384 (1)	9.8 (6)
N2	–0.138 (4)	0.808 (2)	0.111 (2)	25 (1)
Cl	–0.159 (2)	0.559 (2)	0.294 (1)	6.8 (6)
C2	–0.126 (3)	0.715 (2)	0.142 (2)	14 (1)
C3	–0.111 (2)	0.614 (2)	0.175 (2)	7.5 (7)
C4	–0.063 (2)	0.565 (1)	0.099 (1)	5.3 (5)
C11	0.024 (2)	0.252 (1)	0.409 (1)	6.1 (6)
C12	0.108 (2)	0.252 (1)	0.578 (1)	5.2 (6)
C13	0.147 (2)	0.436 (1)	0.386 (1)	4.6 (5)
C14	–0.037 (2)	0.271 (2)	0.642 (2)	7.8 (8)
C15	0.182 (2)	0.498 (1)	0.267 (1)	5.4 (6)
C21	0.072 (2)	0.250 (2)	0.297 (2)	10.6 (7)
C22	0.292 (2)	0.247 (2)	0.104 (2)	10.0 (8)
C23	0.206 (2)	0.062 (1)	0.286 (2)	7.7 (7)
C24	0.333 (2)	0.352 (2)	0.040 (2)	9.5 (9)
C25	0.097 (2)	0.030 (2)	0.256 (2)	9.1 (8)
C31	0.680 (2)	0.295 (1)	0.321 (1)	5.4 (5)
C32	0.484 (2)	0.207 (2)	0.542 (1)	6.6 (6)
C33	0.486 (2)	0.421 (1)	0.410 (1)	6.2 (6)
C34	0.581 (3)	0.227 (2)	0.590 (2)	11.8 (9)
C35	0.510 (2)	0.510 (1)	0.304 (2)	7.2 (7)
C41	0.705 (2)	0.202 (1)	0.290 (1)	5.1 (6)
C42	0.658 (2)	0.264 (1)	0.087 (1)	6.0 (6)
C43	0.586 (2)	0.058 (1)	0.242(1)	5.4 (6)
C44	0.681 (2)	0.379 (2)	0.050 (2)	8.7 (8)
C45·	0.726 (2)	0.017 (2)	0.209 (1)	6.6 (6)
C51	0.5554	0.1208	0.9113	5.7 (9)*
C52	0.4182	0.0356	0.9780	3.9 (7)*
C53	0.6478	0.0834	0.9324	12 (2)*
C61	0.6386	0.2285	0.8320	8 (1)*
N62	0.7004	0.3088	0.7731	12*

[a] Parameters with an asterisk were refined isotropically. Anisotropically refined atoms are given in the form of the isotropic equivalent thermal parameter defined as isotropic equivalent thermal parameters defined as $({}^4/_3)[a^2B(1,1) + (b^2B(2,2) + c^2B(3,3) + ab(\cos\gamma)B(1,2) + ac(\cos\beta)B(1,3) + bc(\cos\alpha)B(2,3)]$.

in, and the red color of the solution turned to yellow. The reaction mixture was placed in an autoclave, reacted with 50 bar of CO_2, and stirred at 50 °C for 16 h. The color of the solution turned to dark yellow. Diethyl ether was added carefully while stirring slowly, and the resulting yellow-brown crystals were collected by filtration, washed with diethyl ether, and dried in vacuo. The analytical and spectroscopical data are summarized in Tables I–VI. For an X-ray analysis, crystals of 1 were prepared by adding diethyl ether at –10 °C to a benzonitrile solution by vapor diffusion.

Preparation of Complex 4. $HIr(PMe_3)_4$ (0.666 g, 1.34 mmol) was dissolved in 10 mL of THF, a solution of malonodinitrile (0.0884 g, 1.34 mmol) in 10 mL of THF was stirred in, and the mixture was transferred to an autoclave. CO_2 was added up to a pressure of 50 bar, and the mixture was stirred for 16 h at a temperature of 50 °C. A white suspension of 4 was isolated from the autoclave, and the solids were collected by filtration, washed with small portions of diethyl ether, and dried in vacuo. Crystals of 4 were obtained by cooling the mother liquor to –20 °C. The analytical and spectroscopical data for 4 are shown in Tables I–VI.

Preparation of Complex 5. $HIr(PMe_3)_4$ (0.83 g, 1.67 mmol) was dissolved in 10 mL of THF. A solution of malonodinitrile (0.108 g, 1.63 mmol) in 10 mL of THF was added slowly. After being stirred for some minutes the solution starts to become cloudy. After 6 h the reaction mixture was cooled to –78 °C. The resulting white solids were collected and dried in vacuo. A second crop was obtained by adding diethyl ether to the mother liquor by vapor diffusion. The analytical and spectroscopical data of 5 are shown in Tables I–VI.

Preparation of Complex 6. $[Ir(depe)_2]Cl$ (0.540 g, 0.84 mmol) was dissolved in 10 mL of benzonitrile. A solution of malonodinitrile (0.0557 g, 0.84 mmol) in 10 mL of benzonitrile was slowly stirred in, and the red color of the solution turned to yellow. After 16 h at room temperature diethyl ether was added slowly, and after the mixture was left standing overnight, yellow-brown crystals of 6 precipitated. They were collected by filtration, washed with diethyl ether, and dried in vacuo. The analytical data of 6 are shown in Tables I–VI.

Collection of Diffraction Data for Compound 1 (and Compound 4). A colorless fragment (light yellow tablet) was mounted in a glass capillary tube and centered on a goniometer. Diffraction data were collected on an Enraf-Nonius CAD-4 automated diffractometer. A triclinic cell was indicated from 25 centered reflections found in the region 15° < 2θ < 20°. The unit cell parameters listed in Tables VIII and IX are refined by least-squares calculations from 25 (29) centered reflections in the range of 25° < 2θ < 35° (39° < 2θ < 45°).

Diffraction data were collected in the hemisphere $\pm h,\pm k,-l$ ($\pm h,\pm k,\pm l$) under the conditions specified in Table VII. Three reflections chosen as intensity standards were monitored every 2 h and showed a decay of 12% in 38 h (71% in 104 h). The crystal was checked for orientation after every 200 reflections and recentered if necessary. Psi scans with nine reflections having 80° < χ < 0° were performed to provide empirical correction for absorption. After correction for Lorentz–polarization effects, absorption, and anisotropic decay, the data sets were averaged.

Solution and Refinement of the Structures of Compound 1 (and Compound 4). The solution of the structures was straightforward from application of the heavy-atom methods. In a three-dimensional Patterson function the Ir atoms were located. The positions of the remaining non-hydrogen atoms were obtained from subsequent difference Fourier calculations. All non-hydrogen atoms are refined anisotropically except the atoms of a half

Table IX. Positional Parameters of Complex 4 and Their Estimated Standard Deviations[a]

atom	*x*	*y*	*z*	*B*, Å^2
Ir	0.25221 (5)	0.61647 (5)	0.30984 (4)	2.90 (1)
P1	0.2706 (4)	0.4152 (4)	0.2219 (3)	4.04 (8)
P2	0.1990 (4)	0.7577 (4)	0.4430 (3)	4.21 (8)
P3	0.1462 (4)	0.7198 (4)	0.1796 (3)	3.83 (8)
P4	0.4824 (3)	0.7082 (4)	0.2960 (3)	3.91 (8)
O1	0.643 (1)	−0.037 (1)	0.074 (1)	5.5 (3)
O2	0.553 (1)	0.152 (1)	0.048 (1)	5.3 (2)
N1	0.897 (1)	0.031 (1)	0.274 (1)	6.2 (3)
N2	0.740 (1)	0.404 (1)	0.205 (1)	5.7 (3)
C1	0.825 (1)	0.085 (1)	0.225 (1)	4.3 (3)
C2	0.737 (1)	0.294 (1)	0.192 (1)	3.8 (3)
C3	0.734 (1)	0.155 (1)	0.168 (1)	3.8 (3)
C4	0.638 (1)	0.090 (1)	0.094 (1)	4.2 (3)
C11	0.353 (2)	0.396 (2)	0.104 (2)	7.5 (5)
C12	0.105 (2)	0.321 (2)	0.191 (2)	7.2 (5)
C13	0.360 (2)	0.302 (2)	0.290 (2)	9.3 (6)
C21	0.179 (2)	0.933 (2)	0.432 (1)	5.9 (4)
C22	0.322 (2)	0.766 (2)	0.550 (1)	6.8 (5)
C23	0.042 (2)	0.706 (2)	0.503 (2)	9.3 (6)
C31	0.200 (2)	0.891 (2)	0.161 (1)	5.3 (4)
C32	−0.040 (1)	0.723 (2)	0.192 (2)	6.7 (5)
C33	0.157 (2)	0.652 (2)	0.050 (1)	6.7 (4)
C41	0.560 (1)	0.686 (2)	0.175 (1)	5.1 (4)
C42	0.608 (2)	0.638 (2)	0.378 (1)	6.3 (4)
C43	0.523 (2)	0.883 (2)	0.326 (2)	6.6 (5)

[a] Anisotropically refined atoms are given in the form of the isotropic equivalent thermal parameter defined as $(^4/_3)[a^2B(1,1) + b^2B(2,2) + c^2B(3,3) + ab(\cos\gamma)B(1,2) + ac(\cos\beta)B(1,3) + bc(\cos\alpha)B(2,3)]$.

molecule of benzonitrile situated around the center of symmetry (0.5, 0, 0) in compound 1. The positions of the hydrogen atoms were calculated by using distances of 148 pm for Ir–H, 95 pm for C–H, and 85 pm for O–H. Full-matrix least-squares refinements of the term $\sum_w(|F_o| - |F_c|)^2$ finally converged with $R = \sum(||F_o| - |F_c||)/\sum|F_o| = 0.041$ (0.050), $R_w = [\sum_w(|F_o| - |F_c|)^2/\sum_w F_o^2]^{1/2} = 0.053$ (0.061), and GOF $= [\sum(|F_o| - |F_c|)^2/(N_o - N_v)]^{1/2}$. Details are listed in Table VII.

Results

The metalation and subsequent carboxylation of activated alkanes has been described for electron-rich iron[10] and iridium complexes.[11] The resulting carboxylate complexes were not isolated, and only spectroscopical data in solution are available. Starting from Herskovitz' work at Du Pont[11] we tried to isolate stable products from the reaction of activated alkanes and CO$_2$. Instead of acetonitrile, which has a pK_a value of 25,[17] the more acidic and therefore more reactive malonodinitrile (pK_a = 12[17]) was used. The iridium complexes [Ir(depe)$_2$]Cl, [Ir(dmpe)$_2$]Cl, and HIr(PMe$_3$)$_4$ and the rhodium complex [Rh(dmpe)$_2$]Cl with the strongly electron-donating ligands dmpe, depe, and PMe$_3$ were chosen. In these ligands the differences between mono- and chelating bis(phosphines) and the steric influences of the alkyl substituents on the phosphorus atoms can be studied.

Reaction of [Ir(depe)$_2$]Cl with Malonodinitrile and CO$_2$. [Ir(depe)$_2$]Cl reacts with malonodinitrile and carbon dioxide to give the yellow brown complex salt 1 (eq 3).

$$[\mathrm{Ir(depe)_2]Cl} + \mathrm{CH_2(CN)_2} + \mathrm{CO_2} \rightarrow \underset{1}{[\mathrm{HIr(depe)_2Cl}]^+[\mathrm{O_2CCH(CN)_2}]^-} \quad (3)$$

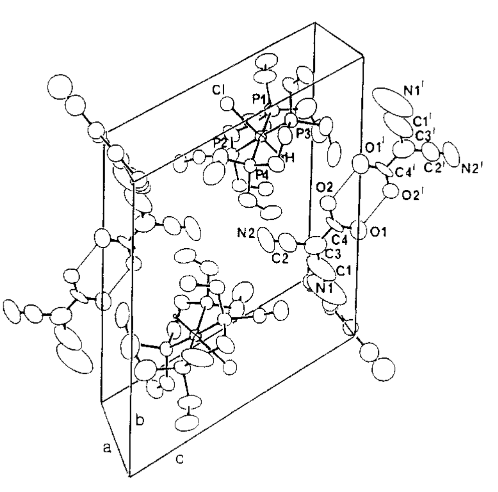

Figure 1. Unit cell of complex 1 (hydrogen atoms omitted for clarity). Only the most important atom labels are given. Two molecules of benzonitrile are enclosed in the structure.

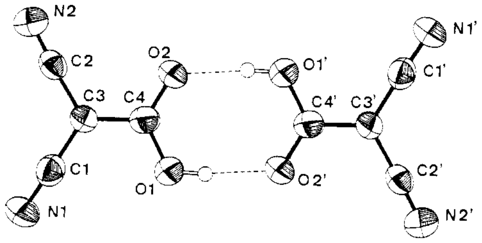

Figure 2. Structure of the dimeric dicyanoacetate anions, view perpendicular to the best plane through all atoms.

The IR spectrum of 1 (Table III) shows bands that were assigned to an Ir–H vibration and to the dicyanoacetate anion. The ^{1}H NMR spectrum at room temperature (Table IV) shows a quintet at −22.35 ppm with a cis P–H coupling constant of 12.8 Hz supporting a square-planar configuration of the two depe ligands. The phosphorus atoms are magnetically equivalent. The trans position of the hydrogen atom must be occupied by a chlorine atom whose low trans effect causes the high-field ^{1}H NMR signal and the high IR oscillation frequency at 2116 cm^{-1}.[18] The two different substituents on both sides of the phosphorus plane cause different ^{1}H NMR absorptions for the ligand protons. The methyl groups of the depe ethyl ligands absorb as two triplets at 0.95 and 1.13 ppm. This shows the magnetic nonequivalence of the methyl groups. The same splitting into two signals can be seen for the methylene and the bridging protons.

The ^{13}C NMR spectrum (Table V) confirms the postulated structure. The signals of the dicyanoacetate anion appear at 171.0, 122.6, and 30.3 ppm. The ligand carbon atoms show more complex absorption patterns because of the coupling with the cis and trans phosphorus atoms. The bridging carbon atoms show a quintet absorption; the methylene carbon atoms show a doublet of a distorted quintet with a coupling constant of 166 Hz. The methyl groups absorb as two singlets with no phosphorus–carbon coupling. The fact that there is a missing P–C coupling for β-C atoms in phosphorus ligands has been described for Pd–phosphine complexes before.[19] The ^{31}P NMR spectrum (Table VI) consists of one peak at 29.18 ppm, which shows the magnetic equivalence of the four phosphorus atoms and confirms the postulated square-planar configuration of the depe ligands.

---

(17) Cram, D. J. *Fundamentals of Carbanion Chemistry*; Academic: New York, 1965.

(18) (a) Chatt, J.; Coffey, R. S.; Shaw, B. L. *J. Chem. Soc.* **1965**, 7391. (b) Ibekwe, S. D.; Taylor, K. A. *J. Chem. Soc. A* **1970**, 1.

(19) (a) Pregosin, P. S.; Kunz, R. *Helv. Chim. Acta* **1975**, *58*, 423. (b) Balimann, G.; Pregosin, P. S. *J. Magn. Reson.* **1976**, *22*, 235. (c) Balimann, G.; Motschi, H.; Pregosin, P. S. *Inorg. Chim. Acta* **1977**, *23*, 191.

The structure of **1** has been verified by X-ray analysis[20] (Tables VII and VIII). Figure 1 shows an ORTEP plot of the elemental cell, which consists of two molecules of **1** and one molecule of benzonitrile, which was used as a solvent. Of special interest is the structure of the dicyanoacetate anions (Figure 2). They are dimeric, with a very short O–O distance of 253 (1) pm, similar to the O–O distances found in dimeric carboxylic acids,[21] which implies the existence of hydrogen atoms between the two O atoms. Carbon atom C3 has sp^2 hybridization with bond angles of about 120° between its three neighbor atoms, C1, C2, and C4. The iridium atom has an octahedral coordination with a square-planar surrounding of the phosphorus atoms and the hydrogen and chlorine atoms in trans position. The acidic proton of the dicyanoacetate anion (formula A, eq 4) was not observed in the ^1H NMR spectrum. Instead a small peak at 3.35 ppm indicates the existence of a methyne proton (formula B, eq 4). This contrast can be explained by a possible proton migration between different isomers of the dicyanoacetate anion. In solution the equilibrium is shifted to compound B with a proton at carbon atom C3. In the crystal form the proton migrates to the oxygen atom giving an anionic carboxylic acid (compound A).

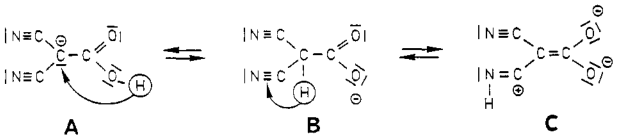

(4)

Reaction of [M(dmpe)$_2$]Cl (M = Ir, Rh) with Malonodinitrile and CO$_2$. Analogous to [Ir(depe)$_2$]Cl, [Ir(dmpe)$_2$]Cl reacts with malonodinitrile and carbon dioxide (eq 5). The IR spectrum of **2** (Table III) shows the bands

$$[Ir(dmpe)_2]Cl + CH_2(CN)_2 + CO_2 \rightarrow \underset{\mathbf{2}}{[HIr(dmpe)_2Cl]^+[O_2CCH(CN)_2]^-} \quad (5)$$

of the dicyanoacetate anion and Ir–H vibrations at 2109 and 2083 cm^{-1}. The ^1H NMR spectrum, measured at room temperature, shows three signals in the offset region: a doublet of multiplets at −14.50 and −15.05 ppm and a quintet at −22.73 ppm (Table IV). When the temperature is increased to 100 °C, the multiplets disappear and the quintet becomes more intense. The signal pattern in the methyl region consists of a doublet of the dmpe methyl protons and a multiplet of the methylene protons, which changes to a distorted triplet at 100 °C. These observations show the existence of cis and trans isomers of the iridium complex. The absorptions at −14.5 and −15.05 ppm are caused by a hydride trans to a phosphorus atom, which can be seen by the chemical shift and the large coupling constant of 110 Hz. The signal at −22.73 ppm shows a hydridic proton trans to a chlorine atom. At higher temperatures the thermodynamically more stable trans position is preferred. The mixture of cis and trans complexes can also be observed in the ^{13}C NMR spectrum (Table V). At room temperature strong signals of the trans isomer at 10.2, 17.6, and 28.1 ppm can be seen. The cis isomer shows weak multiplets at 15.7, 23.1, and 29.5 ppm, which disappear at a temperature of 100 °C.

The rhodium complex **3** can be obtained when [Rh(dmpe)$_2$]Cl is reacted with malonodinitrile and CO_2 (eq 6). The IR spectrum (Table III) shows the expected dicyanoacetate bands and a Rh–H vibration at 2080 cm^{-1}.

$$[Rh(dmpe)_2]Cl + CH_2(CN)_2 + CO_2 \rightarrow \underset{\mathbf{3}}{[HRh(dmpe)_2Cl]^+[O_2CCH(CN)_2]^-} \quad (6)$$

In the ^1H NMR spectrum, measured at room temperature (Table IV), the rhodium hydride shows a quintet absorption at −18.47 ppm that is split into a doublet by the rhodium–hydride coupling of 24.16 Hz. The methyl region shows an intense singlet of the methyl protons and a slightly broadened singlet of the methylene protons. A weak signal at 3.35 ppm and a broad one at 9.93 ppm can be assigned to the different isomers of the dicyanoacetate anions in solution. There is no evidence for a mixture of cis and trans isomers. The ^{13}C NMR spectrum (Table V) agrees with the proposed structure. The signals of the dicyanoacetate anion are similar to the signals of complexes **1** and **2**. The ligand carbon atoms give rise to three quintet absorptions at 27.97, 17.00, and 11.70 ppm. The assignment of these signals was made by a SEFT NMR spectrum ($\tau = 1/J$; 8 μs).[22] The negative phase of the signals at 17.00 and 11.70 ppm shows them to belong to the methyl substituents of the dmpe ligand. The signals of the dicyanoacetate anion show positive signal phases which identify them as quaternary carbon atoms, enclosed carbon atom C3 (cf. Figure 1). This is more evidence for the proton migration in the anion (cf. eq 4) because a hydrogen atom at carbon atom C3 would cause a negative signal phase because of the tertiary character of the carbon in that case. The ^{31}P NMR spectrum of **3** (Table VI) consists of a doublet with a rhodium–phosphorus coupling constant of 89 Hz. This shows the four phosphorus atoms to be magnetically equivalent.

Reaction of HIr(PMe$_3$)$_4$ with Malonodinitrile and CO$_2$. The complexes [Ir(depe)$_2$]Cl, [Ir(dmpe)$_2$]Cl, and [Rh(dmpe)$_2$]Cl react with almost all polar solvents. Benzonitrile with no acidic protons is suitable as a solvent in the reactions with malonodinitrile and CO_2, but it was always enclosed in the products. On the contrary, HIr(PMe$_3$)$_4$ is soluble and stable in most organic solvents. Therefore, the reaction of HIr(PMe$_3$)$_4$ with malonodinitrile and CO_2 was carried out in THF and yielded a white suspension of **4** (eq 7). The IR spectrum of **4** (Table III)

$$HIr(PMe_3)_4 + CH_2(CN)_2 + CO_2 \rightarrow \underset{\mathbf{4}}{[H_2Ir(PMe_3)_4]^+[O_2CCH(CN)_2]^-} \quad (7)$$

shows the bands of the dicyanoacetate anion and two Ir–H vibrations at a lower frequency as in complexes **1** and **2**, which implies that the hydride atoms must be trans to phosphorus atoms.[18] The ^1H NMR spectrum (Table IV) shows a doublet of two distorted triplets at −12.79 and −13.29 ppm with a coupling constant of 99.2 Hz. The low-field absorption and the shape of the signal confirm that the complex is octahedral with a distorted tetrahedral structure of the four phosphorus ligands and the two hydrogen atoms cis to each other.[23] The methyl region shows a doublet assigned to the cis methyl groups and a distorted triplet assigned to the trans methyl groups.[24] The ^{13}C

---

[20] Computer programs used: Schmidt, R. E.; Birkhahn, M.; Massa, W.; Herdtweck, E. STRUX II, Program system for the computation of X-ray data; University Marburg, 1980; Technische Universität München, 1985.

[21] (a) Kanters, J. A.; Kroon, J. *Acta Crystallogr., Sect. B: Struct. Crystallogr. Cryst. Chem.* **1972**, *B28*, 1946. (b) Kanters, J. A.; Roelofsen, G.; Feenstra, T. *Acta Crystallogr., Sect. B: Struct. Crystallogr. Cryst. Chem.* **1976**, *B32*, 3331. (c) Leiserowitz, L.; vor der Brück, D. *Cryst. Struct. Commun.* **1975**, *4*, 647.

[22] Benn, R.; Günther, H. *Angew. Chem., Int. Ed. Engl.* **1983**, *95*, 390.

[23] Meakin, P.; Muetterties, E. L.; Jesson, J. P. *J. Am. Chem. Soc.* **1973**, *95*, 75.

[24] (a) Goodfellow, R. G. *J. Chem. Soc., Chem. Commun.* **1968**, 114. (b) Jenkins, J. M.; Shaw, B. L. *J. Chem. Soc. A* **1966**, 770.

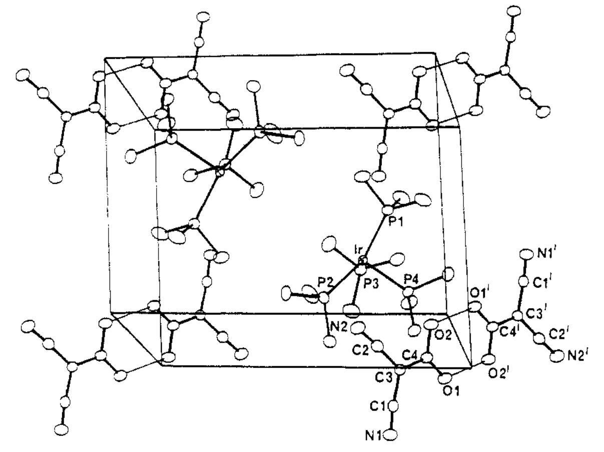

Figure 3. Unit cell of complex 4 (hydrogen atoms omitted for clarity). Only the most important atom labels are given.

NMR spectrum (Table V) gives the signals of the anion as described before. The PMe_3 carbon atoms absorb as a triplet of the trans phosphorus groups and a filled doublet of the cis phosphorus groups.[25] The existence of two different groups of magnetically equivalent phosphorus ligands is confirmed by the ^{31}P NMR spectrum (Table VI), which exhibits two triplets at −51.33 and −57.33 ppm. This pattern is further evidence for the postulated distorted tetrahedral structure of the phosphorus ligands.[23]

The structure of complex **4** has been confirmed by X-ray analysis[20] (Tables VII and IX). Figure 3 shows an ORTEP plot of the elemental cell. The dicyanoacetate anions are dimeric with an O–O distance of 261 (1) pm which is similar to that of **1** (cf. Figure 2).

The results obtained with malonodinitrile as activated hydrocarbon led us to carry out some experiments with acetonitrile as a substrate, but in all cases only unstable products or mixtures were produced. IR and ^{13}C NMR spectra show the existence of carboxylate complexes, but no crystals could be isolated.

Discussion

Complexes **1**–**4** are examples in which a C–C coupling of CO_2 and an activated alkane took place. A proposal for the mechanism of this reaction is exhibited in Figure 4. In path A the activated alkane R–H adds oxidatively to the complex L_nM, yielding a hydrido–alkyl species. Carbon dioxide inserts into the metal–carbon bond, and the resulting carboxylate intermediate is then converted into the product caused by the electron-attracting group R. Another possibility is shown in path B. A proton is abstracted by the complex L_nM giving a hydridic cation and a carbanion, which reacts with the electrophilic carbon atom of CO_2 under C–C coupling to give the carboxylate anion $RCOO^-$. This combines with the hydridic cation yielding the isolated product.

To study the mechanism in more detail, the complex $HIr(PMe_3)_4$ was reacted only with malonodinitrile. After some minutes the light brown complex **5** precipitates (eq 8). The IR spectrum (Table III) shows bands at 2156,

$$HIr(PMe_3)_4 + CH_2(CN)_2 \rightarrow \underset{\mathbf{5}}{[H_2Ir(PMe_3)_4]^+[CH(CN)_2]^-} \qquad (8)$$

2115, and 2086 cm⁻¹ assigned to the nitrile vibrations and at 2055 and 2023 cm⁻¹ assigned to Ir–H vibrations. In contrast to the IR spectrum of **4** the bands at 1612 and 1330 cm⁻¹ are missing. The ^1H NMR spectrum of **5** (Table IV) is similar to the spectrum of **4**. The ^{13}C NMR spectrum (Table V) gives the same signals of the ligand carbon atoms as in complex **4**. Of interest is a strong signal at −1.9 ppm and a change of the nitrile signal from 123.2 ppm (in **4**) to 130.2 ppm (in **5**). These data are similar to the ^{13}C NMR data of the sodium salt of malonodinitrile described in the literature as −2.0 and 130.0 ppm.[26] The ^{31}P NMR spectrum of **5** (Table VI) shows the same triplets at −57.37 and −51.35 ppm as the spectrum of **4**. These results identify complex **5** as a C–H activation product with the composition shown in eq 8. An analogous reaction was performed with $[Ir(depe)_2]Cl$, producing complex **6**. The analytical data (Tables I–VI) show it to have the formula as written in eq 9.

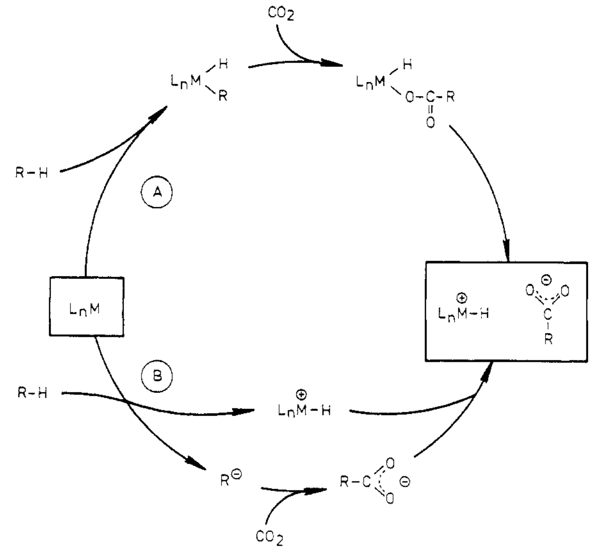

Figure 4. Possible mechanisms for the reaction of activated alkanes with carbon dioxide.

$$[Ir(depe)_2]Cl + CH_2(CN)_2 \rightarrow \underset{\mathbf{6}}{[HIr(depe)_2Cl]^+[CH(CN)_2]^-} \qquad (9)$$

To distinguish between path A and path B (Figure 4), **5** was reacted with CO_2. The coupling of the malonodinitrile anion with carbon dioxide proceeds fast and under mild conditions. Bubbling carbon dioxide through a solution of **5** results in the complete conversion of **5** into complex **4**, which is confirmed by the ^{13}C NMR spectrum. After the reaction the peaks of the malonodinitrile anion at −1.9 and 130.2 ppm have changed and the known peaks of the dicyanoacetate anion at 171.3, 122.7, and 30.5 ppm occur. These results confirm that a C–C coupling of the C–H acidic malonodinitrile with carbon dioxide proceeds via path B in Figure 4.

Acknowledgment. We wish to thank the Deutsche Forschungsgesellschaft and the Bundesminister für Forschung und Technologie for support of this work. A generous gift of iridium trichloride and rhodium trichloride by the Degussa AG (Hanau) is gratefully acknowledged. We also thank B. Dederichs for NMR data and W. Falter for MS data.

Registry No. **1**, 106678-20-0; $1 \cdot {}^1/_2C_7H_5N$, 109909-20-8; **2**, 109909-17-3; **3**, 106678-22-2; **4**, 106707-27-1; **5**, 109909-18-4; **6**, 109909-19-5; $[Ir(depe)_2]Cl$, 60314-46-7; $[Ir(dmpe)_2]Cl$, 60314-45-6; $[Rh(dmpe)_2]Cl$, 16884-41-6; $HIr(PMe_3)_4$, 83380-16-9; $CH_2(CN)_2$, 109-77-3; CO_2, 124-38-9.

---

(25) Redfield, D. A.; Nelson, J. H.; Cary, L. W. *Inorg. Nucl. Chem. Lett.* **1974**, *10*, 727.

(26) Kalinowski, H. O.; Berger, S.; Braun, S. *^{13}C NMR Spektroskopie*, Thieme Verlag: Stuttgart, 1984.

Supplementary Material Available: Atom labeling schemes and tables of final atomic positional parameters, final thermal parameters, and interatomic distances and angles of the compounds 1 and 4 and root-mean-square amplitudes for 1 and least-squares planes for 4 (27 pages); listings of structure factors for 1 and 4 (30 pages). Ordering information is given on any current masthead page. Further details of the crystal structure investigation are available on request from the Fachinformationszentrum Energie, Physik, Mathematik GmbH, D-7514 Eggenstein-Leopoldshafen 2, by quoting the depository numbers CSD 52345 (complex 1) and CSD 52020 (complex 4), the names of the authors, and the journal citation.

Silylene Reactions with Ethylene and Butadiene: Mechanism and Kinetics

D. S. Rogers, K. L. Walker, M. A. Ring,* and H. E. O'Neal*

Department of Chemistry, San Diego State University, San Diego, California 92182

Received November 18, 1986

The reactions of SiH_2 (generated from the disilane pyrolysis) with ethylene and with butadiene have been studied by the comparative rate technique. Ethylene trapping of silylene is a consecutive step process involving the formation of a silacyclopropane intermediate which can react back to reactants or forward to either ethylsilylene or vinylsilane. Reaction products of ethylene trapping vary with reaction conditions. At high reactant concentrations and low temperatures the main product is ethylsilane, but numerous other products including diethylsilane and ethyldisilane are also formed. At low reactant concentrations and moderate temperatures the main products are ethylsilane and vinylsilane, while at high temperatures vinylsilane is the only significant product. A number of rate constants and rate-constant parameters for the relevant reactions of the proposed rather complex mechanism have been estimated by using a variety of data sources (including the present paper), and the reaction system has been modeled with reasonable success over a wide range of pressure and temperature conditions.

Introduction

Reactions of silanes with olefins are known to produce the corresponding alkylsilanes; however, under some conditions other products are also produced. Thus Fritz et al.[1] found that silane and ethylene reacted at $T > 380$ °C and atmospheric pressures to produce, in addition to ethylsilane, diethylsilane, triethylsilane, and traces of higher molecular weight products. Rochow and White,[2] in a similar study (456–511 °C) found (besides ethylsilane and diethylsilane) disilane, trisilane, and a product tentatively identified as ethyldisilane. These and other similar results[3,4] were explained in terms of free radical processes (e.g. Scheme I type reactions).

Scheme I. Free Radical Mechanism for Silane–Ethylene Reactions

$$SiH_4 \xrightarrow{1} SiH_3^\bullet + H^\bullet$$

$$SiH_3^\bullet + C_2H_4 \xrightarrow{2} SiH_3CH_2CH_2^\bullet$$

$$SiH_3CH_2CH_2^\bullet + SiH_4 \xrightarrow{3} SiH_3^\bullet + C_2H_5SiH_3$$

$$C_2H_5SiH_3 \xrightarrow{4} C_2H_5SiH_2^\bullet + H^\bullet$$

$$C_2H_5SiH_2^\bullet + C_2H_4 \xrightarrow{5} C_2H_5SiH_2CH_2CH_2^\bullet$$

$$C_2H_5SiH_2CH_2CH_2^\bullet + SiH_4 \xrightarrow{6} (C_2H_5)_2SiH_2 + SiH_3^\bullet$$

etc.

Scheme II. Silylene Mechanism for Silane–Ethylene Reactions

$$SiH_4 + (M) \xrightarrow{7} :SiH_2 + H_2 + (M)$$

$$:SiH_2 + C_2H_4 \xrightarrow{8} C_2H_5\ddot{Si}H$$

$$C_2H_5\ddot{Si}H + SiH_4 \xrightarrow{9} C_2H_5SiH_2SiH_3$$

$$C_2H_5SiH_2SiH_3 \xrightarrow{10} C_2H_5SiH_3 + :SiH_2$$

$$C_2H_5\ddot{Si}H + C_2H_4 \xrightarrow{11} (C_2H_5)_2Si:$$

$$(C_2H_5)_2Si: + SiH_4 \xrightarrow{12} (C_2H_5)_2SiHSiH_3$$

$$(C_2H_5)_2SiHSiH_3 \xrightarrow{13} (C_2H_5)_2SiH_2 + SiH_2:$$

etc.

However, it is now clear that silylenes and not free radicals are the dominant intermediates of these reactions and that their mechanism is better represented as shown in Scheme II. Observations which support the Scheme II interpretation are as follows:

(1) Silane–olefin reaction only occur at temperatures where silane itself thermally decomposes.[1]

(2) Silane–olefin reactions have rates that are very comparable to those of the initial step of the silane pyrolysis, inferring an initiation of the former by the latter.[5]

(3) The major initiation reactions of silane and alkylsilane pyrolyses are 1,1-H_2 elimination reactions producing silylenes.[6]

---

* To whom reprint requests should be addressed.

[1] Fritz, G. *Z. Naturforsch.*, B: *Chem., Biochem., Biophys. Biol.* **1952**, *7B*, 207.

[2] White, D. G.; Rochow, E. G. *J. Am. Chem. Soc.* **1954**, *76*, 3897.

[3] Sawrey, B. A.; O'Neal, H. E.; Ring, M. A. *Int. J. Chem. Kinet.* **1984**, *16*, 23.

[4] Neudorfl, P. S.; Strausz, O. P. *J. Phys. Chem.* **1978**, *82*, 241.

[5] Erwin, J. W.; Ring, M. A.; O'Neal, H. E. *Int. J. Chem. Kinet.* **1985**, *17*, 1067.

0276-7333/87/2306-2313$01.50/0